Iranian Journal of Mathematical Chemistry



DOI: 10.22052/IJMC.2025.255596.1915 Vol. 16, No. 4, 2025, pp. 313-336 Research Paper

A Family of Amplified 3-Step Störmer Methods for Solving the Schrödinger Equation and its Related Problems

Sanaz Hami Hassan Kiyadeh¹, Ramin Goudarzi Karim², Ali Safaie³, Somayeh Darabi⁴, Fayyaz Khodadosti⁵ and Hosein Saadat⁶

Keywords:

Initial value problems (IVPs), Störmer methods, Complex amplifier, Periodic and orbital problems, Amplification factor, Phase lag

AMS Subject Classification (2020):

65L05: 65L06

Article History:

Received: 10 October 2024 Accepted: 12 March 2025

Abstract

A family of complex amplified Störmer methods is studied for solving initial value problems of second-order differential equations with periodic or orbital solutions. The new complex amplified Störmer methods depend upon a parameter w>0, vanish its complex amplifier, and integrate precisely algebraic polynomials. We believe that each method category (Störmer method is one of them) has its complex amplifier. When finding the coefficients of the Störmer methods, if the imaginary and real parts of the complex amplifier, if necessary, their derivatives are equal to zero, high-capability methods are obtained.

The principal local truncation errors of the new explicit Störmer methods are addressed. Their stability regions are depicted in a plane where the vertical axis is the problem frequency and the Horizontal axis is the method frequency. A collection of numerical examples illustrates the success of the new family of complex amplified Störmer methods in addressing the Schrödinger equation and other related problems. The advantage of the new methods is showcased by discussing their relevance to some issues in chemistry.

 $\ \, \odot$ 2025 University of Kashan Press. All rights reserved.

E-mail addresses: shkiyadeh@crimson.ua.edu (S. H. Hassan Kiyadeh), rkarim@stillman.edu (R. Goudarzi Karim), alisafaie549@gmail.com (A. Safaie), somayeh-darabi-90@yahoo.com (S. Darabi), fayyaz64dr@gmail.com (F. Khodadosti), h67saadat@gmail.com (H. Saadat)

Academic Editor: Abbas Saadatmandi

¹Department of Mathematics, The University of Alabama, Alabama, USA

²Department of Computational and Information Sciences, Stillman College, Alabama, USA

³Department of Mathematics, Faculty of Basic science, The Khatam-ol-Anbia (PBU) University, Tehran, Iran

⁴Department of Mathematics, Faculty of Mathematical Science, University of Maragheh, Maragheh, Iran

⁵Department of Mathematics, National University of Skills (NUS), Tehran, Iran

⁶Department of Mathematics, The University of Tabriz, Tabriz, Iran

^{*}Corresponding author

1 Introduction

Many problems in chemistry, including quantum chemistry, physical chemistry, and more, are mathematically modeled using second-order ordinary differential equations. Solving these modeled problems has always been a challenge throughout various times. Therefore, ever since the 17th century, second-order initial-value problems as

$$y'' + w^{2}y = \epsilon f(t, y), \quad t_{0} < t \leqslant t_{\text{end}}, \quad w > 0, \quad y \in \mathbb{R}^{n},$$

$$y(t_{0}) = y_{0}, \quad y'(t_{0}) = y'_{0},$$
 (1)

have been solved numerically in the context of chemical phenomena. Where the principal frequency w is known and dominates the disturbance force ϵ ($\epsilon \ll 1$). In this framework, we will consider a coupled differential equations of the Schrödinger type and some IVPs of second-order differential equations. The colse-coupling differential equations of the Schrödinger type as follows:

$$\left[\frac{d^2}{dt^2} + k_i^2 - \frac{l_i(l_i+1)}{t^2}\right] y_{ij}(t) = \sum_{\substack{n=1\\n\neq i}}^N \mathcal{P}(t)_{in} y_{nj}(t), \quad i, j = 1(1)N,$$
 (2)

whose boundary value conditions are given by

$$y_{ij}(0) = 0,$$

$$y_{ij}(t) \approx k_i t \mathcal{J}_{l_i}(k_i t) \theta_{ij} + \left(\frac{k_i}{k_j}\right)^{1/2} K_{ij} k_i t \mathcal{N}_{li}(k_i t),$$
(3)

where $\mathcal{J}_l(x)$ and $\mathcal{N}_l(x)$ are spherical Bessel and Neumann functions, respectively (see for details [1, 2]). Various schemes have been proposed for solving such equations.

The foremost numerical methods in the context of planetary integrations date back to Störmer (1907) introducer of explicit methods, Cowell (1910) introducer of implicit methods, and Jackson (1925) introducer of one-step methods. An improved Cowell's method is inspected by Stiefel and Bettis in [3]. An adaptive Nyström-Cowell-like method with high order is investigated by Franco and Palacian in [4]. In [5], the Störmer-Cowell method with second-sum and the split form is introduced by Frankena. Through numerical examples, the ascendancy of the symmetric 8, 10, and 12-step methods with high-order was presented versus the Störmer methods [6].

Heretofore, there were only a handful of authors who have addressed Störmer methods and specifications of Störmer methods are little known among numerical analysts, let alone the communication with its complex amplifier as an accelerator. Another reason that increases the motivation to address this issue is that the construction and implementation of explicit methods are cost-effective.

The main achievements and contributions can be summarized as follows:

- We begin with a profound study of the complex amplifier corresponding to explicit k-step Störmer methods, which is presented as a theorem.
- Now, to find the coefficients of the new methods, two equations are used: one is the operator related to the method, and the other is the complex amplifier related to the method, which consists of two real and imaginary parts.
- The first method is achieved by zeroing the complex amplifier's real part and integrating algebraic polynomials up to degree 3.

- The second method is obtained by zeroing the real and imaginary parts and integrating the algebraic polynomials up to degree 1.
- The third method is obtained by zeroing both the real and imaginary parts and zeroing the first derivative of the real part, namely the phase lag.

The continuation of the article is as follows: In Section 2, we see how the complex amplifier of the explicit k-step Störmer method is determined in the form of a theorem. In Section 3, we address to principal local truncation error (PLTE) and stability regions of the new complex amplified explicit 3-step Störmer method. In Section 4, we demonstrate the potential of the new family of the amplified explicit 3-step Störmer methods by providing some examples inspired by quantum chemistry and physical chemistry (e.g. the Schrödinger equation). Finally, in Section 5, we mention some significant remarks and outcomes about the amplified explicit 3-step Störmer methods.

2 Derivation of the methods

Unfortunately, the literature shows that the terminology for explicit k-step Störmer methods has been somewhat unconsolidated and loose. Some researchers considered the classical explicit k-step Störmer methods as

$$y(t_n + h) - 2y(t_n) + y(t_n - h) = h^2 \sum_{j=0}^{k} b_j(v) y''(t_n - jh),$$
(4)

where k represents the number of steps and h represents the step-length of the method. The the explicit k-step Störmer method (4) is associated with the following operator

$$\mathcal{L}(y(t),h) = y(t_n + h) - 2y(t_n) + y(t_n - h) - h^2 \sum_{j=0}^{k} b_j(v) y''(t_n - jh),$$
 (5)

where $y \in \mathbb{C}^2 = \mathbb{C} \times \mathbb{C}$, \mathbb{C}^2 is the set of all ordered pairs of complex numbers, and $b_j(v)$ are the coefficients of method that depend on v for all j = 0(1)k. Letting $\epsilon = 0$ in (1) we get the following scalar test equation

$$y'' = -w^2 y, (6)$$

we apply the explicit k-step Störmer method (4) to the scalar test equation (6) and get the following difference equation

$$y(t_n + h) - 2y(t_n) + y(t_n - h) = v^2 \sum_{j=0}^{k} b_j(v)y(t_n - jh),$$
(7)

where v = wh.

The characteristic equation associated to the explicit k-step Störmer method (4) is given as

$$\Omega_k(\lambda, v) = \lambda - 2 + \lambda^{-1} - v^2 \sum_{j=0}^k b_j(v) \lambda^{-j}.$$
 (8)

Definition 2.1. A real analytic function $\theta(v) - v$ has the following Maclaurin series

$$\theta(v) - v = \sum_{j=1}^{\infty} C_j v^j,$$

the term $C_1v^{q+1} + \mathcal{O}(v^{q+2})$ is called the amplification factor of order q with constant C_1 and the term $C_2v^{q+2} + \mathcal{O}(v^{q+3})$ is called the phase-lag of order q with constant C_2 [7].

Lemma 2.2. By trigonometric expansions, the following equation is valid:

$$\sin(j\theta(v)) - \sin(jv) = -jv^{q+1} - \sum_{l=2}^{\infty} C_l v^{q+l},$$
$$\cos(j\theta(v)) - \cos(jv) = j^2 v^{q+2} + \sum_{l=3}^{\infty} C_l v^{q+l},$$

where $\theta(v)$ is theoretical function.

Proof. See [8].

Theorem 2.3. For an explicit k-step Störmer method, complex amplifier is given by

$$CA_k(v) = \frac{2 - 2\cos(v) - v^2 \sum_{j=0}^k b_j(v)\cos(jv)}{\left(2 + v^2 \sum_{j=0}^k b_j(v)j^2\right)} + I \frac{v^2 \sum_{j=0}^k b_j(v)\sin(jv)}{v^2 \sum_{j=0}^k b_j(v)j},$$

where I is imaginary unit.

Proof. We establish $\Omega_k(e^{Ij\theta(v)}, v)$ as

$$\Omega_k(e^{Ij\theta(v)}, v) = e^{I\theta(v)} + e^{-I\theta(v)} - 2 + v^2 \sum_{j=0}^k b_j(v)e^{-Ij\theta(v)} = 0,$$

applying Euler's theorem, we have

$$\left[\cos(\theta(v)) + I\sin(\theta(v)) + \cos(-\theta(v)) + I\sin(-\theta(v))\right] - 2t + v^2 \sum_{j=0}^k b_j(v) \left[\cos(-j\theta(v)) + I\sin(-j\theta(v))\right] = 0,$$

after simplifying, we obtain

$$2\cos(\theta(v)) - 2 + v^2 \sum_{j=0}^{k} b_j(v)\cos(j\theta(v)) - Iv^2 \sum_{j=0}^{k} b_j(v)\sin(j\theta(v)) = 0,$$

we separate the imaginary and real parts and set them equal to zero

Real:
$$2\cos(\theta(v)) - 2 + v^2 \sum_{j=0}^{k} b_j(v)\cos(j\theta(v)) = 0,$$
Imaginary:
$$v^2 \sum_{j=0}^{k} b_j(v)\sin(j\theta(v)) = 0.$$
(9)

According to Definition 2.1, we achieve

$$\begin{cases} 2\cos(v) + 2\left(v^{q+2} + \mathcal{O}\left(v^{q+3}\right)\right) - 2 \\ + v^2 \sum_{j=0}^k b_j(v) \left(\cos(jv) + j^2 v^{q+2} + \mathcal{O}\left(v^{q+3}\right)\right) = 0, \\ v^2 \sum_{j=0}^k b_j(v) \left(\sin(jv) - j\left(v^{q+1} + \mathcal{O}\left(v^{q+2}\right)\right)\right) = 0, \end{cases}$$

by simplifying, the above equation becomes

$$\begin{cases} 2\cos(v) - 2 + v^2 \sum_{j=0}^{k} b_j(v) \cos(jv) = -\left(2 + v^2 \sum_{j=0}^{k} b_j(v) j^2\right) \left(v^{q+2} + \mathcal{O}\left(v^{q+3}\right)\right) = 0, \\ v^2 \sum_{j=0}^{k} b_j(v) \sin(jv) = v^2 \sum_{j=0}^{k} b_j(v) j\left(v^{q+1} + \mathcal{O}\left(v^{q+2}\right)\right) = 0. \end{cases}$$

In the real part, the most effective term is the phase lag, and in the imaginary part, the amplification factor, so we are looking for these two, and we find

$$\begin{cases} \text{ phase lag} = v^{q+2} + \mathcal{O}\left(v^{q+3}\right) = \frac{2 - 2\cos(v) - v^2 \sum_{j=0}^k b_j(v)\cos(jv)}{\left(2 + v^2 \sum_{j=0}^k b_j(v)j^2\right)}, \\ \text{Amplification factor} = v^{q+1} + \mathcal{O}\left(v^{q+2}\right) = \frac{v^2 \sum_{j=0}^k b_j(v)\sin(jv)}{v^2 \sum_{j=0}^k b_j(v)j}, \end{cases}$$

both imaginary and real parts must be added together, and we have:

$$CA_k(v) = \frac{2 - 2\cos(v) - v^2 \sum_{j=0}^k b_j(v)\cos(jv)}{\left(2 + v^2 \sum_{j=0}^k b_j(v)j^2\right)} + I \frac{v^2 \sum_{j=0}^k b_j(v)\sin(jv)}{v^2 \sum_{j=0}^k b_j(v)j}.$$

Therefore, the theorem is proven.

Using the above theorem, the complex amplifier and its first derivative of the real part for

the explicit 3-step Störmer method (4) are given by:

$$\begin{split} \mathcal{C}\mathcal{A}_3(v) = & \frac{2-2\,\cos{(v)} - v^2\,(b_0(v) + b_1(v)\cos{(v)} + b_2(v)\cos{(2\,v)})}{v^2b_1(v) + 4\,v^2b_2(v) + 2} \\ & + I\frac{(b_1(v)\sin{(v)} + b_2\sin{(2\,v)})}{b_1(v) + 2\,b_2(v)}, \\ \Re(\mathcal{C}\mathcal{A}_3(v)) = & \left[\sin{(v)}\,v^4b_1(v)^2 + 4\sin{(v)}\,v^4b_1(v)b_2(v) + 2\sin{(2\,v)}\,v^4b_1(v)b_2(v) \\ & + 8\sin{(2\,v)}\,v^4b_2(v)^2 + 4\sin{(v)}\,v^2b_1(v) + 8\sin{(v)}\,v^2b_2(v) \\ & + 4\,b_2v^2\sin{(2\,v)} + 16\cos{(v)}\,vb_2(v) - 4\,vb_0(v) - 4\cos{(2\,v)}\,vb_2(v) \\ & - 4\,vb_1(v) - 16\,vb_2(v) + 4\sin{(v)}\,\right] \Big/ \Big[\left(v^2b_1(v) + 4\,v^2b_2(v) + 2\right)^2 \Big]. \end{split}$$

2.1 The first method

By solving the following system

$$\{\mathcal{L}(t^2, h) = 0, \ \mathcal{L}(t^3, h) = 0, \ \Re(\mathcal{C}\mathcal{A}_3(v)) = 0\},\$$

three coefficients $b_0(v)$, $b_1(v)$, $b_2(v)$ of the first complex amplified 3-step Störmer method are obtained as:

$$b_{0}(v) = \frac{1}{2} \frac{2 v^{2} (\cos(v))^{2} - 2 \cos(v) v^{2} - v^{2} - 2 \cos(v) + 2}{v^{2} \cos(v) (\cos(v) - 1)},$$

$$b_{1}(v) = \frac{v^{2} + 2 \cos(v) - 2}{v^{2} \cos(v) (\cos(v) - 1)},$$

$$b_{2}(v) = \frac{1}{2} \frac{-v^{2} - 2 \cos(v) + 2}{v^{2} \cos(v) (\cos(v) - 1)}.$$

$$(10)$$

Figure 1 shows curves of the coefficients behavior for the first complex amplified 3-step Störmer method for v = w h from 0 to 50.

Since the value |v| approach to zero, the coefficients (10) of first method are subject to heavy

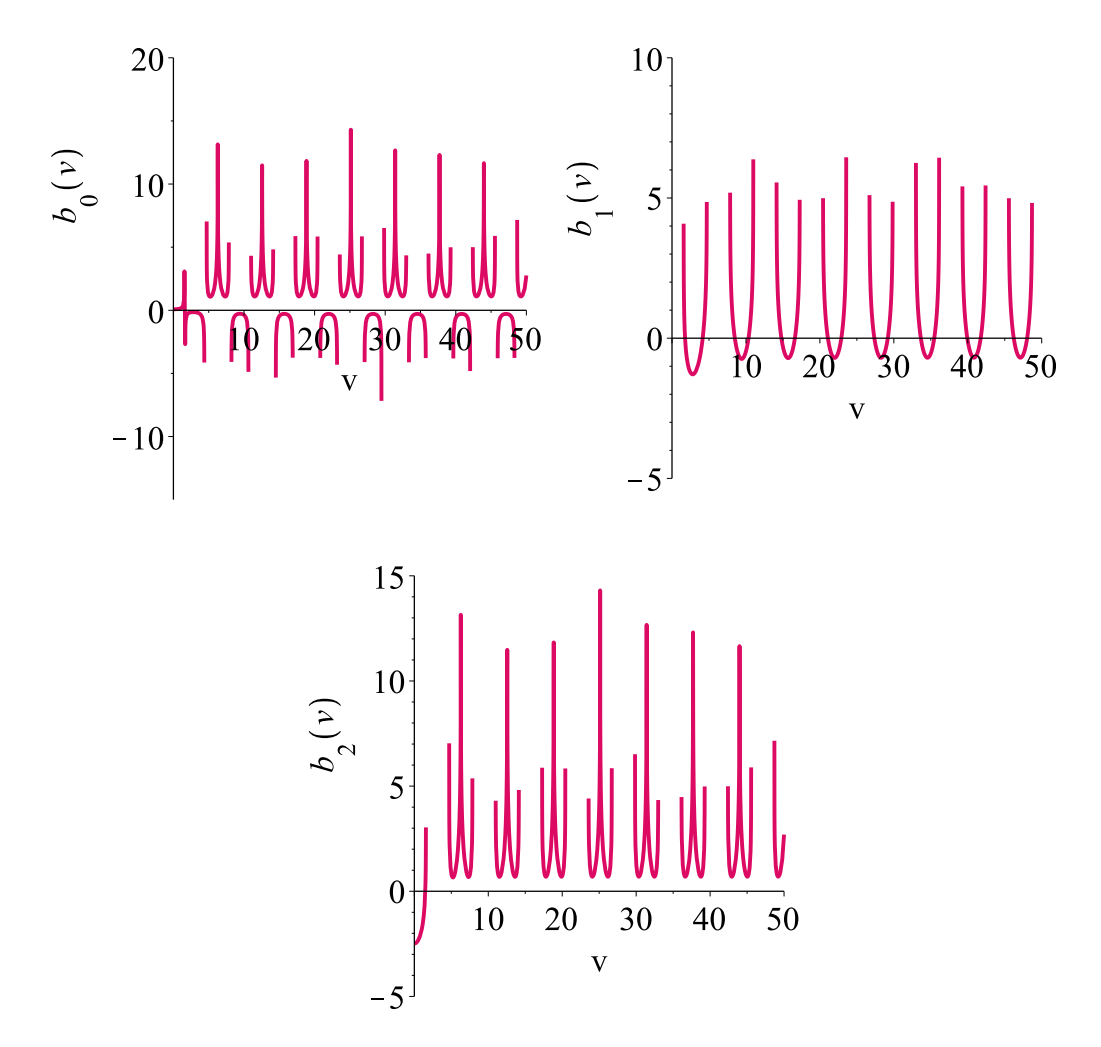


Figure 1: The curves of the coefficient's behavior of the first complex amplified 3-step Störmer method for $v \in [0, 50]$.

cancellations, we use Maclaurin series expansions of them as:

$$b_0(v) = \frac{13}{12} + \frac{11}{240} + \frac{593}{30240} + \frac{9697}{1209600} + \frac{259703}{79833600} + \frac{1724332931}{1307674368000} + \frac{55908779}{104613949440} + \frac{3950804953}{18240380928000} + \frac{448493303575451}{5109094217170944000} + \frac{4080494790726437}{114693951814041600000} + \frac{149103204826715759}{10340806695553990656000} + \frac{9898311611236134768923}{1693824136731743669452800000} + \mathcal{O}(v^{24}),$$

$$b_1(v) = -\frac{1}{6} - \frac{11}{12}v^2 - \frac{593}{15120}v^4 - \frac{9697}{604800}v^6 - \frac{259703}{39916800}v^8 - \frac{1724332931}{653837184000} + \frac{4080494790726437}{52306974720}v^{12} - \frac{3950804953}{9120190464000}v^{14} - \frac{448493303575451}{653837184000} + \frac{4080494790726437}{57346975907020800000} - \frac{149103204826715759}{5170403347776995328000} + \frac{9898311611236134768923}{65383718400000} + \mathcal{O}(v^{24}),$$

$$b_2(v) = \frac{1}{12} + \frac{11}{2}v^2 + \frac{593}{30240}v^4 + \frac{9697}{1209600}v^6 + \frac{259703}{79833600}v^8 + \frac{1724332931}{1307674368000}v^{10} + \frac{55908779}{104613949440}v^{12} + \frac{3950804953}{1209600}v^{14} + \frac{259703}{79833600}v^8 + \frac{1724332931}{1307674368000}v^{10} + \frac{55908779}{104613949440}v^{12} + \frac{3950804953}{18240380928000}v^{14} + \frac{448493303575451}{1307674368000}v^{10} + \frac{4080494790726437}{104613949440}v^{13} + \frac{3950804953}{18240380928000}v^{14} + \frac{448493303575451}{10340806695553990656000}v^{10} + \frac{4080494790726437}{114693951814041600000}v^{13} + \frac{149103204826715759}{10340806695553990656000}v^{20} + \frac{9898311611236134768923}{10340806695553990656000}v^{22} + \frac{9898311611236134768923}{10340806695553990656000}v^{22} + \frac{9898311611236134768923}{10340806695553990656000}v^{22} + \frac{11}{104613949440}v^{13} + \frac{149103204826715759}{10340806695553990656000}v^{22} + \frac{11}{1046139454136731743669452800000}v^{22} + \mathcal{O}(v^{24}).$$

2.2 The second method

By solving the following system

$$\{\mathcal{L}(t^2, h) = 0, \, \mathcal{C}\mathcal{A}_3(v) = 0\}.$$

three coefficients $b_0(v)$, $b_1(v)$, $b_2(v)$ of the second complex amplified 3-step Störmer method are obtained as:

$$b_{0}(v) = \frac{1}{2} \frac{(\cos(v) + 1) \left(4 (\cos(v))^{2} + v^{2} - 6 \cos(v) + 2\right)}{(\sin(v))^{2} v^{2}},$$

$$b_{1}(v) = -\frac{\cos(v) (\cos(v) + 1) \left(v^{2} + 2 \cos(v) - 2\right)}{(\sin(v))^{2} v^{2}},$$

$$b_{2}(v) = \frac{1}{2} \frac{(\cos(v) + 1) \left(v^{2} + 2 \cos(v) - 2\right)}{(\sin(v))^{2} v^{2}}.$$

$$(12)$$

Figure 2 shows curves of the coefficient's behavior for the second complex amplified 3-step Störmer method for v = wh from 0 to 50. For the reasons stated earlier, we use Maclaurin series expansions of the coefficient's behavior for the second complex amplified 3-step Störmer

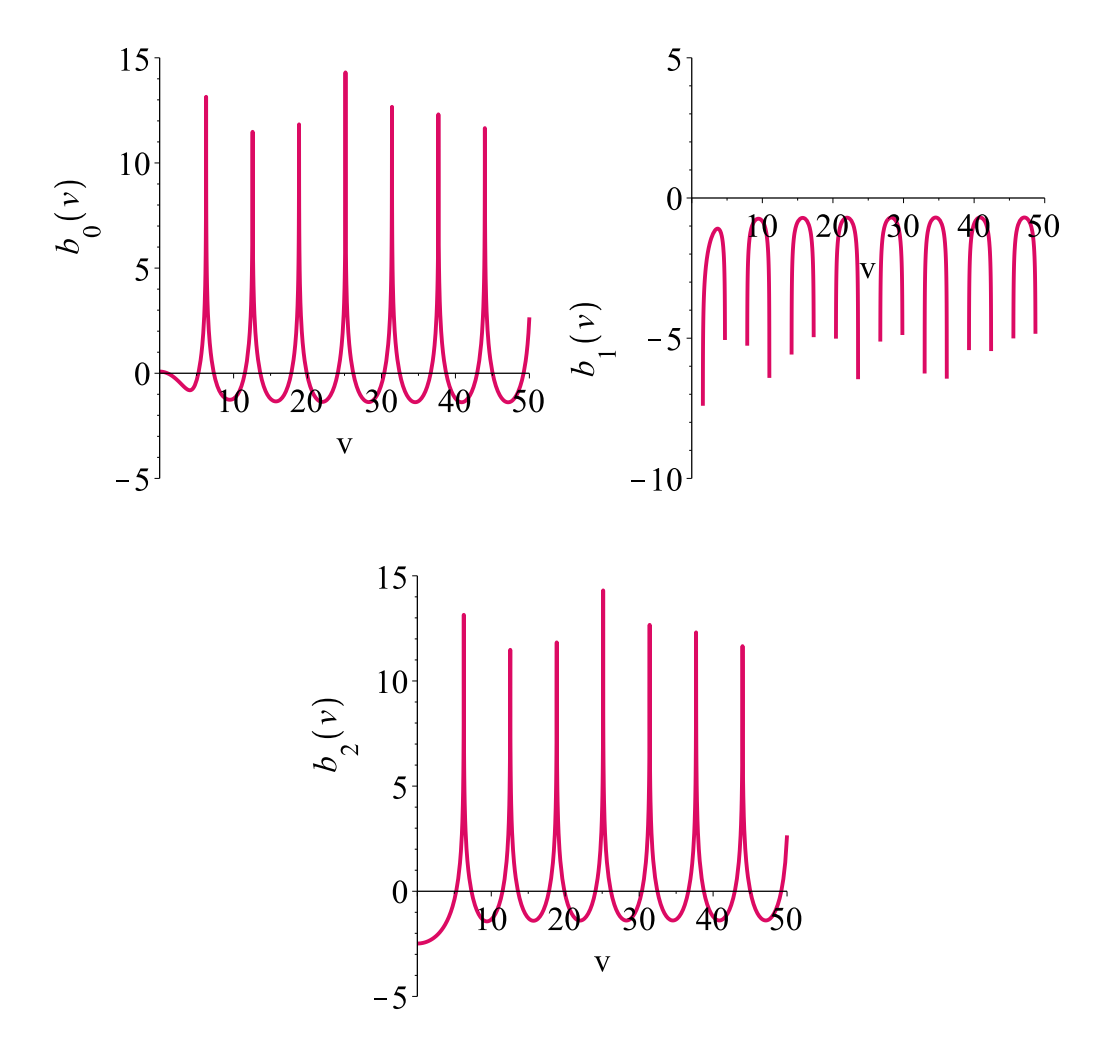


Figure 2: The curves of the coefficient's behavior of the second complex amplified 3-step Störmer method for $v \in [0, 50]$.

method as:

$$b_0(v) = \frac{13}{12} - \frac{19 v^2}{240} + \frac{89 v^4}{30240} - \frac{53 v^6}{1209600} + \frac{59 v^8}{79833600} + \frac{2141 v^{10}}{1307674368000}$$

$$+ \frac{103 v^{12}}{523069747200} + \frac{13 v^{14}}{2605768704000} + \frac{149467 v^{16}}{1021818843434188800}$$

$$+ \frac{3316949 v^{18}}{802857662698291200000} + \frac{5981683 v^{20}}{51704033477769953280000}$$

$$+ \frac{5436368633 v^{22}}{1693824136731743669452800000} + \mathcal{O}(v^{24}),$$

$$b_1(v) = -\frac{1}{6} + \frac{3 v^2}{40} - \frac{47 v^4}{15120} + \frac{23 v^6}{604800} - \frac{37 v^8}{39916800} - \frac{4871 v^{10}}{653837184000}$$

$$- \frac{97 v^{12}}{261534873600} - \frac{3583 v^{14}}{355687428096000} - \frac{67867 v^{16}}{232231555325952000}$$

$$- \frac{473897 v^{18}}{57346975907020800000} - \frac{6173 v^{20}}{26679067841986560000}$$

$$- \frac{5436371363 v^{22}}{846912068365871834726400000} + \mathcal{O}(v^{24}),$$

$$b_2(v) = \frac{1}{12} + \frac{v^2}{240} + \frac{v^4}{6048} + \frac{v^6}{172800} + \frac{v^8}{5322240} + \frac{691 v^{10}}{118879488000}$$

$$+ \frac{v^{12}}{5748019200} + \frac{3617 v^{14}}{711374856192000} + \frac{43867 v^{16}}{300534953951232000}$$

$$+ \frac{174611 v^{18}}{42255666457804800000} + \frac{77683 v^{20}}{671480954256752640000}$$

$$+ \frac{236364091 v^{22}}{73644527683988855193600000} + \mathcal{O}(v^{24}).$$

2.3 The third method

By solving the following system

$$\{\mathcal{CA}_3(v)=0,\ \frac{d}{dv}\Re\left(\mathcal{CA}_3(v)\right)=0\},$$

three coefficient's $b_0(v)$, $b_1(v)$, $b_2(v)$ of the third complex amplified 3-step Störmer method are obtained as:

$$b_{0}(v) = \left[-2 (\cos(v))^{2} + \left(2 v (\sin(v))^{3} - 3 \sin(v) v + 2 \right) \cos(v) - 2 v (\sin(v))^{3} + 2 \sin(v) v \right] / \left[\sin(v) (\cos(v))^{2} v^{3} \right],$$

$$b_{1}(v) = \frac{2 \sin(v) v + 4 \cos(v) - 4}{\sin(v) v^{3}},$$

$$b_{2}(v) = \frac{-\sin(v) v - 2 \cos(v) + 2}{\cos(v) \sin(v) v^{3}}.$$

$$(14)$$

Figure 3 shows curves of the coefficient's behavior for the third complex amplified 3-step Störmer method for v = w h from 0 to 50. For the reasons stated earlier, we use Maclaurin series expansions of the coefficient's behavior for the third complex amplified 3-step Störmer method

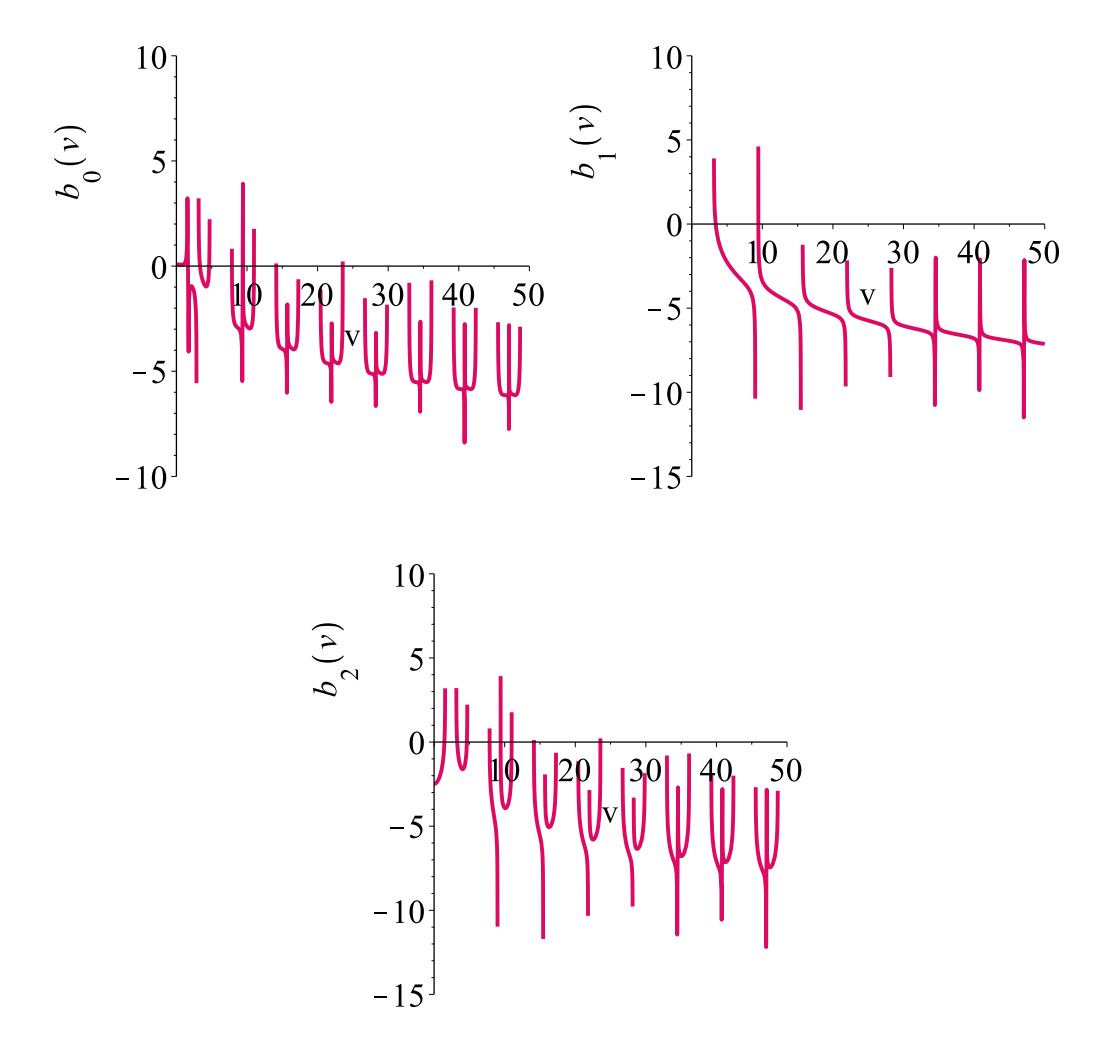


Figure 3: The curves of the coefficient's behavior of the third complex amplified 3-step Störmer method for $v \in [0, 50]$.

as:

$$b_0\left(v\right) = \frac{13}{12} - \frac{1}{30}\,v^2 + \frac{169\,v^4}{6720} + \frac{1679\,v^6}{181440} + \frac{303059\,v^8}{79833600} + \frac{2423\,v^{10}}{1572480} \\ + \frac{6535869943\,v^{12}}{10461394944000} + \frac{45035888581\,v^{14}}{177843714048000} + \frac{1664659390271\,v^{16}}{16219346721177600} \\ + \frac{5838451733911\,v^{18}}{140359731240960000} + \frac{1743293679502451281\,v^{20}}{103408066955539906560000} \\ + \frac{17663265262303613401\,v^{22}}{2585201673888497664000000} + \mathcal{O}\left(v^{24}\right), \\ b_1\left(v\right) = -\frac{1}{6} - \frac{v^2}{60} - \frac{17\,v^4}{10080} - \frac{31\,v^6}{181440} - \frac{691\,v^8}{39916800} - \frac{5461\,v^{10}}{3113510400} \\ - \frac{929569\,v^{12}}{5230697472000} - \frac{3202291\,v^{14}}{177843714048000} - \frac{221930581\,v^{16}}{121645100408832000} \\ - \frac{4722116521\,v^{18}}{25545471085854720000} - \frac{56963745931\,v^{20}}{3041413733986467840000} \\ - \frac{14717667114151\,v^{22}}{77556050216654929920000000} + \mathcal{O}\left(v^{24}\right), \\ b_2\left(v\right) = \frac{1}{12} + \frac{1}{20}\,v^2 + \frac{451\,v^4}{20160} + \frac{211\,v^6}{22680} + \frac{20201\,v^8}{5322240} + \frac{4797553\,v^{10}}{3113510400} \\ + \frac{594169973\,v^{12}}{951035904000} + \frac{833997937\,v^{14}}{3293402112000} + \frac{24969890853989\,v^{16}}{243290200817664000} \\ + \frac{151799745081689\,v^{18}}{3649353012264960000} + \frac{83013984738211957\,v^{20}}{4924193664549519360000} \\ + \frac{1892492706675387151\,v^{22}}{276985893630910464000000} + \mathcal{O}\left(v^{24}\right). \\$$

3 The methods investigation

3.1 Study of the PLTEs

Here, to study the PLTEs of the three new complex amplified 3-step Störmer methods, we write the Taylor series (TS) of the 3-step Störmer method as:

$$TS = (1 - b_{0}(v) - b_{1}(v) - b_{2}(v)) h^{2}y^{(2)}(t) + (b_{1}(v) + 2b_{2}(v)) h^{3}y^{(3)}(t)$$

$$+ \left(\frac{1}{12} - \frac{1}{2}b_{1}(v) - 2b_{2}(v)\right) h^{4}y^{(4)}(t) + \left(\frac{1}{6}b_{1}(v) + \frac{4}{3}b_{2}(v)\right) h^{5}y^{(5)}(t)$$

$$+ \left(\frac{1}{360} - \frac{1}{24}b_{1}(v) - \frac{2}{3}b_{2}(v)\right) h^{6}y^{(6)}(t) + \left(\frac{b_{1}(v)}{120} + \frac{4b_{2}(v)}{15}\right) h^{7}y^{(7)}(t)$$

$$+ \left(\frac{1}{20160} - \frac{b_{1}(v)}{720} - \frac{4b_{2}(v)}{45}\right) h^{8}y^{(8)}(t) + \left(\frac{b_{1}(v)}{5040} + \frac{8b_{2}(v)}{315}\right) h^{9}y^{(9)}(t) + \mathcal{O}\left(h^{10}\right).$$

$$(16)$$

By placing the coefficients (11) in the above expansion, all terms up to the 4th order in h become zero, and the PLTE for the first complex amplified 3-step Störmer method and its classical partner are obtained as follows:

$$PLTE_{Classic} = PLTE_{First} = \frac{1}{12}h^5y^{(5)}.$$

Table 1: The periodicity interval of the new complex amplified 3-step Störmer methods.

Method	Periodicity interval
Classical method	1.76
First method	1.41
Second method	2.88
Third method	1.52

By placing the coefficients (13) and (15) in the above expansion, all terms up to the 2th order in h become zero, and the PLTE for the second, and third complex amplified 3-step Störmer methods are obtained as follows:

$$PLTE_{Second} = PLTE_{Third} = PLTE_{Classic} + \frac{1}{12}h^5w^2y^{(3)}.$$

3.2 Depicting of stability regions

In order to sketch the region of stability, we apply all of the new complex amplified k-step Störmer method to the test equation

$$y''(t) = -\tau^2 y(t),$$
 (17)

by applying the family of phase-fitted 3-step Störmer methods to the scalar test equation in (17), eventually, we obtain the following characteristic polynomial

$$\Omega(v, s, \xi) = \rho(\xi) - s^{2}\sigma(v, \xi),$$

$$\rho(\xi) = \xi^{k-2} (\xi^{2} - 2\xi + 1),$$

$$\sigma(v, \xi) = \sum_{j=0}^{k} b_{j}(v) \xi^{j},$$
(18)

where $v = \omega h$ and $s = \tau h$.

Definition 3.1. An explicit k-step Störmer method (4) has a periodicity interval as $(0, s_0^2)$ if all roots of the characteristic equation (18) satisfy the root-conditions given as

$$\xi_{1,2} = e^{\pm I\theta(s)}, |\xi_i| \le 1, \quad i = 3(1)k - 1, \quad \forall s < s_0,$$
 (19)

where $s = \tau h$ and I is imaginary unit (see [7]).

Letting v = s and scrolling from zero with a step length of 0.01 toward the point where the roots of the characteristic equation (18) no longer satisfy the root-conditions (19), we obtain the periodic interval of the new complex amplified 3-step Störmer methods. Table 1 represents the periodicity interval of the new complex amplified 3-step Störmer methods. According to Table 1, the stability interval for the second method has increased remarkably.

Definition 3.2. A stability region of an explicit k-step Störmer method (4) encompasses the regions of the s-v plane that at each point like (\mathbf{s}, \mathbf{v}) all roots of the characteristic equation (18) satisfy the root-conditions given (19).

Figures 4 to 6 represent the stability regions of the new complex amplified 3-step Störmer methods are visualized using purple color, and in white colors, the new complex amplified 3-step Störmer methods are instability regions.

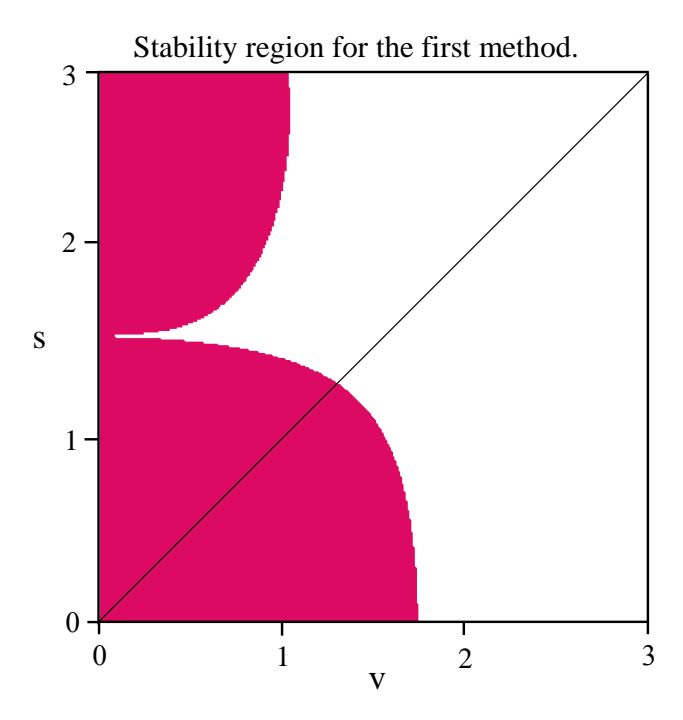


Figure 4: The stability region of the first complex amplified 3-step Störmer method.

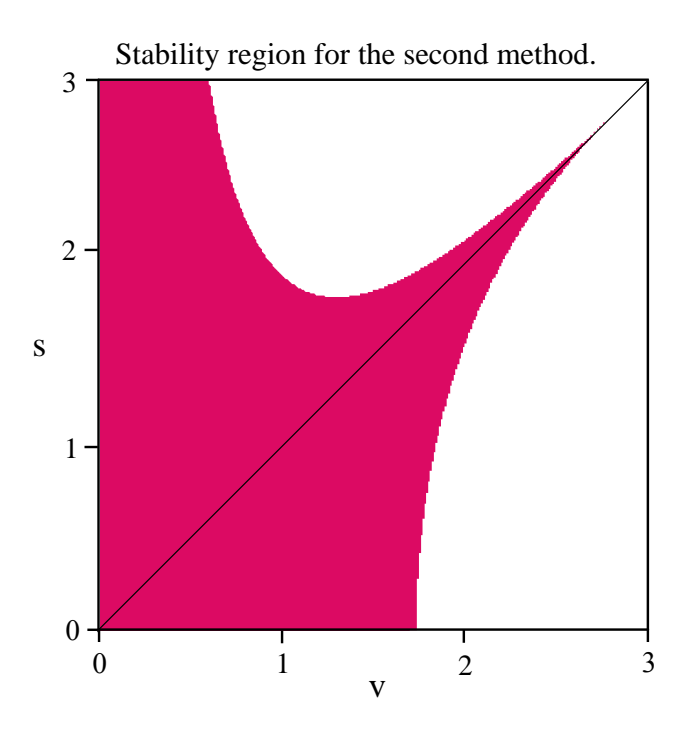


Figure 5: The stability region of the second complex amplified 3-step Störmer method.

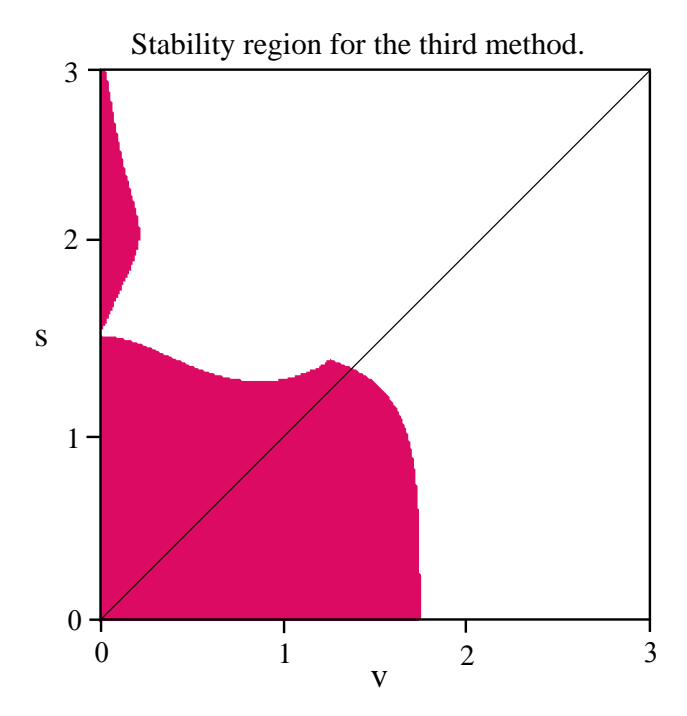


Figure 6: The stability region of the third complex amplified 3-step Störmer method.

We circumscribe the stability region of the new complex amplified 3-step Störmer methods to the upper right quadrant. Since the coefficients of the new complex amplified 3-step Störmer methods depend on v and the problems depend on s, we take $v \in [0,3]$ and $s \in [0,3]$. In Figures 4 to 6 the vertical axis is s and the horizontal axis is v.

4 Numerical specimens

Using a 6-order Runge-Kutta-Nyström schemes, computed some starting values. We assume that all frequencies are equal. The accuracy of the methods is obtained as follows:

Accuracy =
$$-\log_{10} \left(\max \left(\text{Error} \left(y_i \left(t \right) \right) \right) \right)$$
,

$$\text{Error} \left(y_i \left(t \right) \right) = \left| y_i \left(t \right)_{\text{Num}} - y_i \left(t \right)_{\text{Exact}} \right|, \quad i = 1(1)N,$$
(20)

where N is the dimension of the system of second-order IVPs.

All computations were performed on a PC with a 2.6 GHz processor, using Matlab version 2013a in double-precision arithmetic.

4.1 Some explicit multi-step methods

In the handful of articles that compared classical explicit k-step Störmer methods with other methods, we selected some methods for comparison and listed them below.

• **Second**: The second explicit complex amplified 3-step Störmer method of fourth algebraic order presented in the Section 3.

- Third: The third explicit complex amplified 3-step Störmer method of fourth algebraic order presented in the Section 3.
- First: The first explicit complex amplified 3-step Störmer method of fourth algebraic order presented in the Section 3.
- Class: The original explicit 3-step Störmer method of fourth algebraic order presented in the Section 3.
- Quin10: The symmetric 10-step method of fourteenth algebraic order presented in the Section 2 of [6].
- Quin8: The symmetric 8-step method of twelfth algebraic order presented in the Section 2 of [6].
- Lamb6: The symmetric 6-step method of tenth algebraic order by taking a = 0 presented in the Section 3 of [7].
- Lamb4: The symmetric 4-step method of eighth algebraic order by taking a = 0 presented in the Section 3 of [7].

4.2 Some problems in the field of chemistry

In this part, we display five second-order IVPs to estimate the accuracy of the new explicit complex amplified 3-step Störmer methods.

Example 4.1. The generalized famous Bessel's equation is the first example as

$$y''(t) = -\left(\eta^2 b^2 t^{2(b-1)} + \frac{1 - 4a^2 b^2}{4t^2}\right) y(t), \quad y(1) = J_a(\eta), \ t \ge 1, \tag{21}$$

whose theoretical solution is given by

$$y(t) = t^{\frac{1}{2}} J_a \left(\eta t^b \right),$$

where J_a is the Bessel function of the first kind of order a. For this example, we select b=1, a=0, and take different values for η i.e. $\eta \in [10,30]$.

The Equation (21) is solved when $t \in [1,600]$ and h = 1/40. The accuracy lines of the methods versus CPU time for solving the IVP (21) are presented in Figure 7. As the frequency of the Bessel's equation increases and approaches 30 in Figure 7 related to Equation (21), all methods lose their accuracy except for two methods. One of them is the third new method, which has acceptable accuracy by increasing η up to about 17. The second new method preserves the accuracy and almost no drop in accuracy is observed with increasing frequency.

Example 4.2. An inhomogeneous equation is the second example as

$$y''(t) = -\eta^2 y(t) + (\eta^2 - 1)\sin(t), \quad y(0) = 0, \ y'(0) = \eta + 1, \tag{22}$$

whose theoretical solution is given by

$$y(t) = \cos(\eta t) + \sin(\eta t) + \sin(t).$$

For this example, we take different values for η i.e. $\eta \in [10, 30]$.

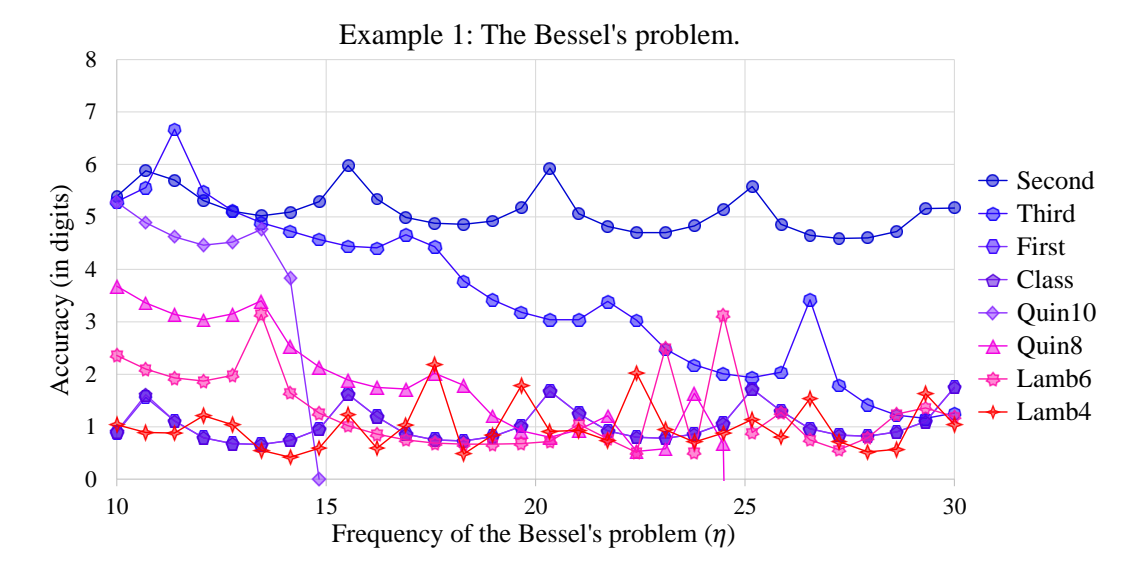


Figure 7: Curves of the accuracy of the methods versus increasing the frequency of the problem in Example 4.1.

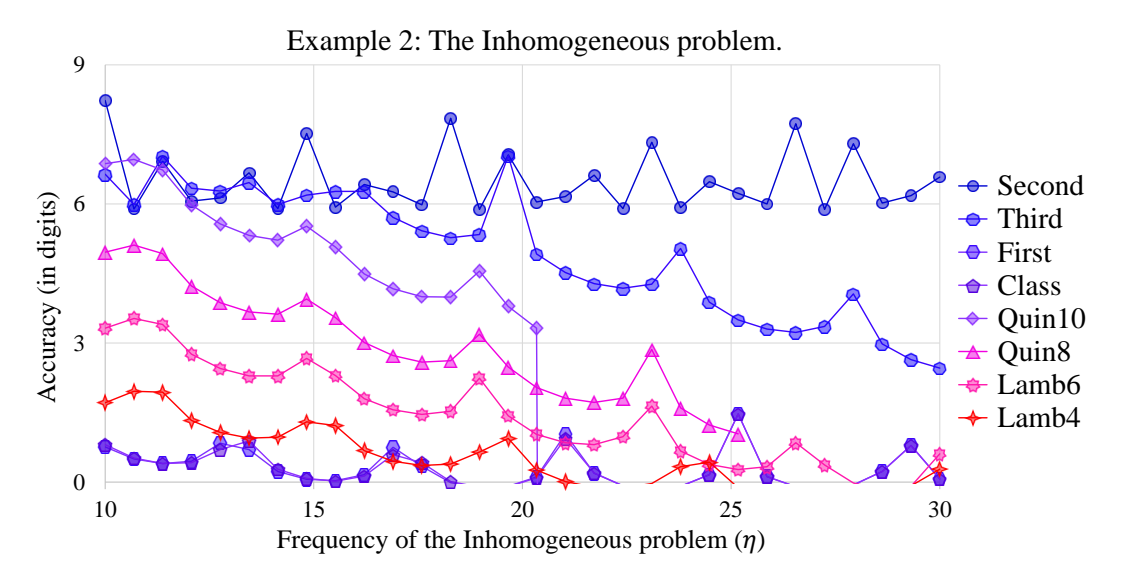


Figure 8: Curves of the accuracy of the methods versus increasing the frequency of the problem in Example 4.2.

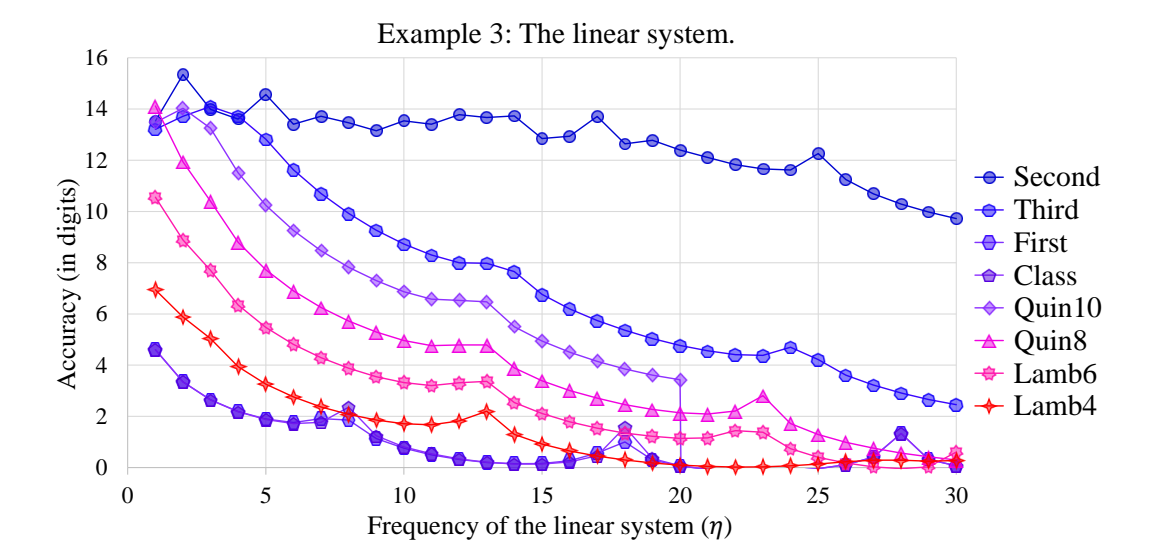


Figure 9: Curves of the accuracy of the methods versus increasing the frequency of the problem in Example 4.3.

The Equation (22) is solved when $t \in [0,300]$ and h = 1/30. The accuracy lines of the methods versus CPU time for solving the IVP (22) are presented in Figure 8. In Figure 8, the accuracy of all methods has a significant slowdown with increasing frequency. The third new method presented here is as accurate as the second method up to the frequency of 20, but approaching 30, the third method has meaningful accuracy.

Example 4.3. We consider generalized stiff second-order linear system investigated by Franco et al. [9]:

$$y_{1}''(t) = -\left(\frac{\eta^{2}}{2} + r\right)y_{1}(t) + \left(\frac{\eta^{2}}{2} - r\right)y_{2}(t), \quad y_{1}(0) = -1, \quad y_{1}'(0) = -\eta,$$

$$y_{2}''(t) = + \left(\frac{\eta^{2}}{2} - r\right)y_{1}(t) - \left(\frac{\eta^{2}}{2} + r\right)y_{2}(t), \quad y_{2}(0) = +1, \quad y_{2}'(0) = +\eta,$$

$$(23)$$

whose theoretical solution is

$$y_1(t) = -\left(\cos\left(\eta t\right) + \sin\left(\eta t\right)\right),$$

$$y_2(t) = \cos\left(\eta t\right) + \sin\left(\eta t\right).$$

For this example, we select $r = \pi$ and take different values for η i.e. $\eta \in [0, 30]$.

The system of IVPs (23) is solved when $t \in [0, 200]$ when h = 1/35. The accuracy lines of the methods versus CPU time for solving the IVPs (23) are presented in Figure 9. In Figure 9, it is widely seen that no method is accurate with increasing frequency, except for our second new method, although we see a slight drop in the accuracy curve with increasing frequency.

Example 4.4. A second-order linear system of IVPs studied by Lambert and Watson [7]:

$$y_{1}''(t) = -\eta^{2}y_{1}(t) + g''(t) + \eta^{2}g(t), \ y_{1}(0) = \alpha + g(0), \ y_{1}'(0) = g'(0),$$

$$y_{2}''(t) = -\eta^{2}y_{2}(t) + g''(t) + \eta^{2}g(t), \ y_{2}(0) = g(0), \ y_{2}'(0) = \eta \alpha + g'(0),$$

$$(24)$$

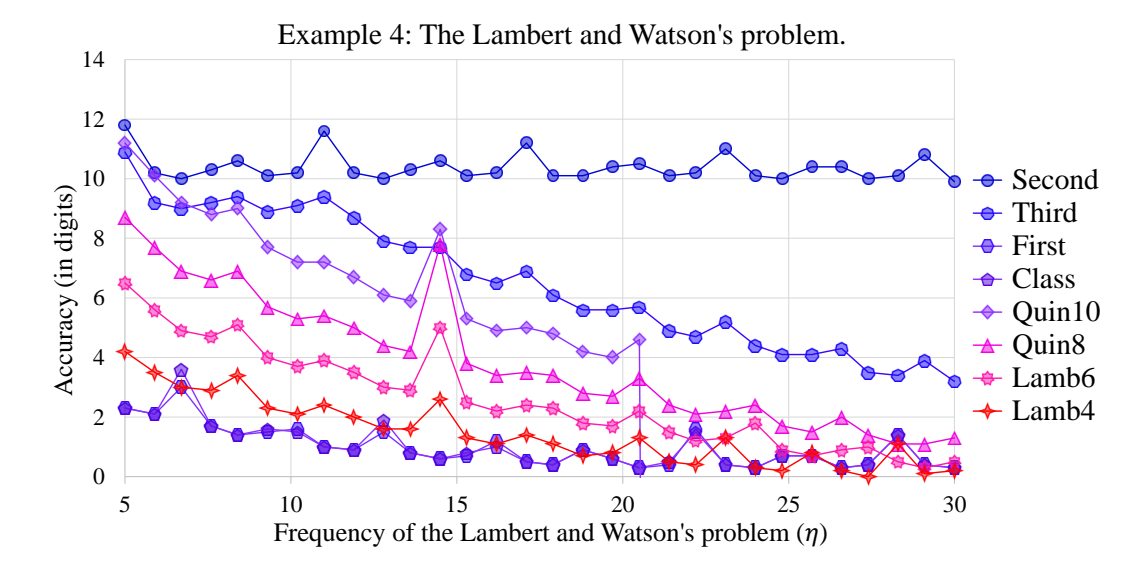


Figure 10: Curves of the accuracy of the methods versus increasing the frequency of the problem in Example 4.4.

whose theoretical solution is given by

$$y_1(t) = \alpha \cos(\eta t) + g(t),$$

$$y_2(t) = \alpha \sin(\eta t) + g(t),$$

where $g(t) = e^{-t/20}$. In this example, we select $\alpha = 0.1$ and take different values for η i.e. $\eta \in [0, 30]$.

The Equation (24) is solved over $t \in [0, 200]$ when h = 1/35. The accuracy lines of the methods versus CPU time for solving the IVPs (24) are presented in Figure 10. In Figure 10, again, this is the second method of the methods presented in this article, which has maintained its accuracy with increasing frequency of the problem.

Example 4.5. The fifth our problem is a generalized second-order linear system studied by Kramarz as [10]:

$$y_1''(t) = (r - 2\eta^2) y_1(t) + (2r - 2\eta^2) y_2(t), \quad y_1(0) = 2, \quad y_1'(0) = -\eta, y_2''(t) = (\eta^2 - r) y_1(t) + (\eta^2 - 2r) y_2(t), \quad y_2(0) = -1, \quad y_2'(0) = +\eta,$$
(25)

whose theoretical solution is given by

$$y_1(t) = 2\cos(\eta t),$$

 $y_2(t) = -\cos(\eta t).$

We select r = 100 and take different values for η i.e. $\eta \in [0, 30]$.

The Equation (25) is solved over $t \in [0, 200]$ when h = 1/35. The accuracy lines of the methods versus CPU time for solving the IVPs (25) are presented in Figure 11. In Figure 10, according to the previous examples, the second method is more accurate with increasing frequency.

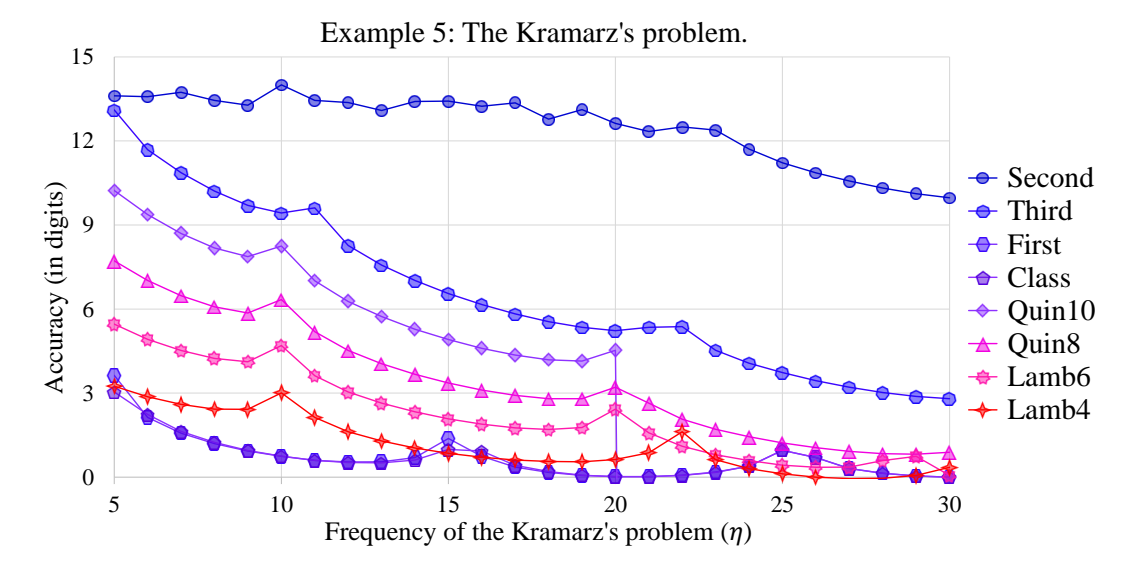


Figure 11: Curves of the accuracy of the methods versus increasing the frequency of the problem in Example 4.5.

Example 4.6. We consider an unperturbed harmonic oscillator system as:

$$y_1''(t) = -\eta^2 y_1(t), \quad y_1(0) = 1, \quad y_1'(0) = -\eta, y_2''(t) = -\eta^2 y_2(t), \quad y_2(0) = 0, \quad y_2'(0) = +\eta,$$
(26)

whose theoretical solution is given by

$$y_1(t) = 2\cos(\eta t),$$

$$y_2(t) = -\cos(\eta t).$$

We take different values for η i.e. $\eta \in [5, 30]$.

The Equation (26) is solved over $t \in [0, 400]$ when h = 1/35. The accuracy lines of the methods versus CPU time for solving the IVPs (26) are presented in Figure 12. Figure 12 shows that the accuracy curve of all methods drops rapidly with increasing frequency. The second new method presented is more accurate despite increasing the problem frequency.

Example 4.7. We consider high-frequency nonlinear system studied by Franco [11]:

$$y_{1}''(t) = -\eta^{2}y_{1}(t) + \frac{2y_{1}(t)y_{2}(t) - \sin(2\eta t)}{\left(y_{1}(t)^{2} + y_{2}(t)^{2}\right)^{\frac{3}{2}}}, \quad y_{1}(0) = 1, \quad y_{1}'(0) = 0,$$

$$y_{2}''(t) = -\eta^{2}y_{2}(t) + \frac{y_{1}(t)^{2} - y_{2}(t)^{2} - \cos(2\eta t)}{\left(y_{1}(t)^{2} + y_{2}(t)^{2}\right)^{\frac{3}{2}}}, \quad y_{2}(0) = 0, \quad y_{2}'(0) = \eta,$$

$$(27)$$

whose theoretical solution is given

$$y_1(t) = \cos(\eta t),$$

$$y_2(t) = \sin(\eta t).$$

We take different values for η i.e. $\eta \in [5, 30]$.

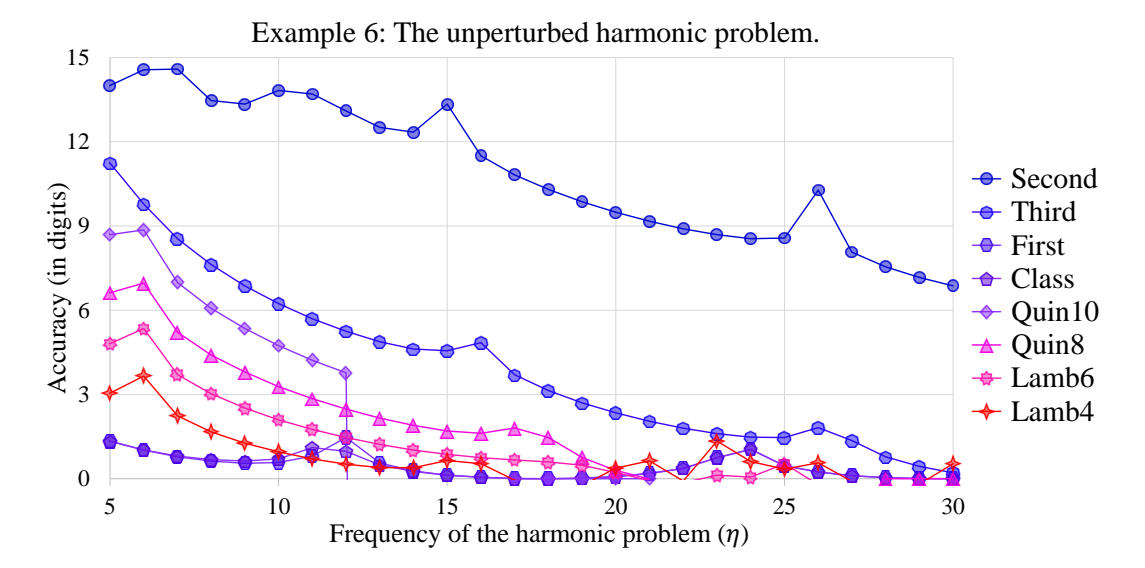


Figure 12: Curves of the accuracy of the methods versus increasing the frequency of the problem in Example 4.6.

The Equation (27) is solved over $t \in [0, 200]$ when h = 1/35. The accuracy lines of the methods versus CPU time for solving the IVPs (27) are presented in Figure 13. Figure 13 also shows that, except for the second new method, all methods are declining with increasing frequency.

Example 4.8. Rotational excitation of a diatomic molecule by neutral particle impact is one problem in quantum chemistry that may be described in terms of coupled differential equations. We assume that the entrance channel is indicated by the quantum numbers (j,l), the exit channels are indicated by (j',l'), and the total angular momentum is indicated by J=j+l=j'+l'. In this case, we achieve

$$\left[\frac{d^2}{dt^2} + k_{j'j}^2 - \frac{l'(l'+1)}{t^2}\right] y_{j'l'}^{Jjl}(t) = \frac{2v}{\hbar^2} \sum_{j''} \sum_{l''} \langle j'l'; J | \mathcal{P}(t) | j''l''; J \rangle y_{j''l''}^{Jjl}(t), \tag{28}$$

with

$$k_{j'j} = \frac{2\nu}{\hbar^2} \left[E + \frac{\hbar^2}{2I} \left\{ j(j+1) - j'(j'+1) \right\} \right],$$

where E is the kinetic energy of the incident particle in the center-of-mass system, $\mathcal{P}(t)$ is potential which can be expressed as a combination of two potential functions $V_0(t)$ and $V_2(t)$, I is the moment of inertia of rotator, $\langle j'l'; J|\mathcal{P}(t)|j''l''; J\rangle$ is coupling matrix, $k_{j'j}$ is the wave vector, and ν is the reduced mass of the system (see for details [1, 2]). To present numerical results, we consider the following parameters

$$\frac{2\nu}{\hbar^2} = 1000.0, \quad \frac{\nu}{I} = 2.351, \quad E = \eta,
V_0(t) = \frac{1}{t^{12}} - 2\frac{1}{t^6}, \quad V_2(t) = 0.2283V_0(t).$$
(29)

We assume J=6 and consider excitation of the rotator from the j=0 state to levels up to

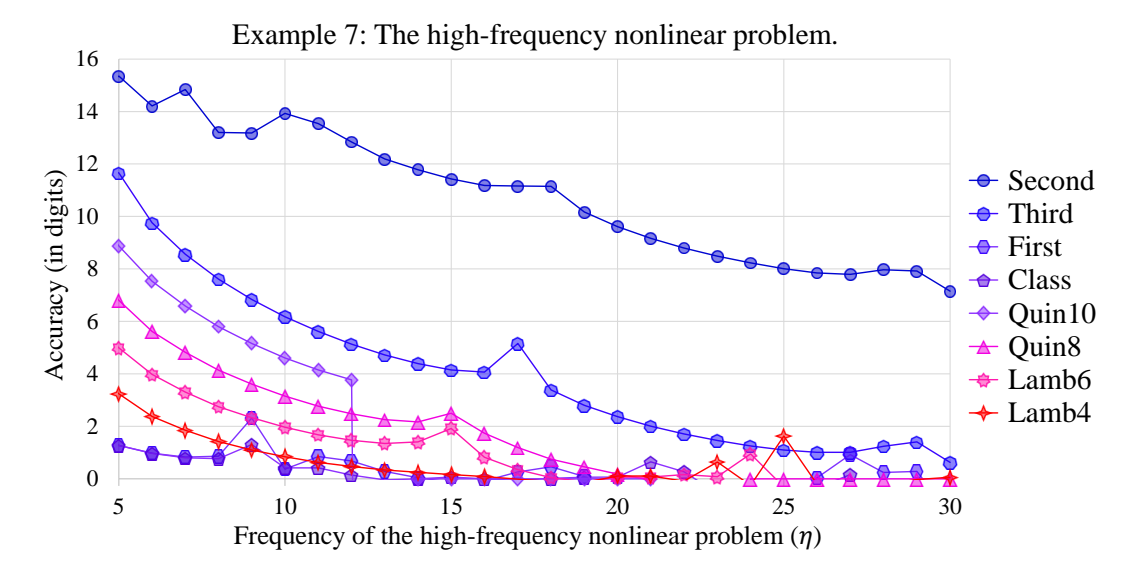


Figure 13: Curves of the accuracy of the methods versus increasing the frequency of the problem in Example 4.7.

j'=2,4,6 giving rise to sets of 4, 9, and 16 coupled equations, respectively. We take different values for η i.e. $\eta \in [5,25]$.

The Equation (28) is solved over $t \in [0, 50]$. The accuracy lines of the methods versus CPU time for solving the IVPs (28) are presented in Figure 14.

5 Conclusion

The explicit k-step Stormer methods were out of the spotlight, and since we believe every method category has a complex/real boost to overcome high-frequency problems [12, 13]. We found complex amplifiers for these methods. Using this amplifier, we presented three new methods. The final result is that we will have a low-cost method if the real and imaginary parts are zero when finding the coefficients.

Conflicts of Interest. The authors declare that they have no conflicts of interest regarding the publication of this article.

Acknowledgments. The authors would like to thank the anonymous reviewers for their helpful comments that greatly improved the manuscript.

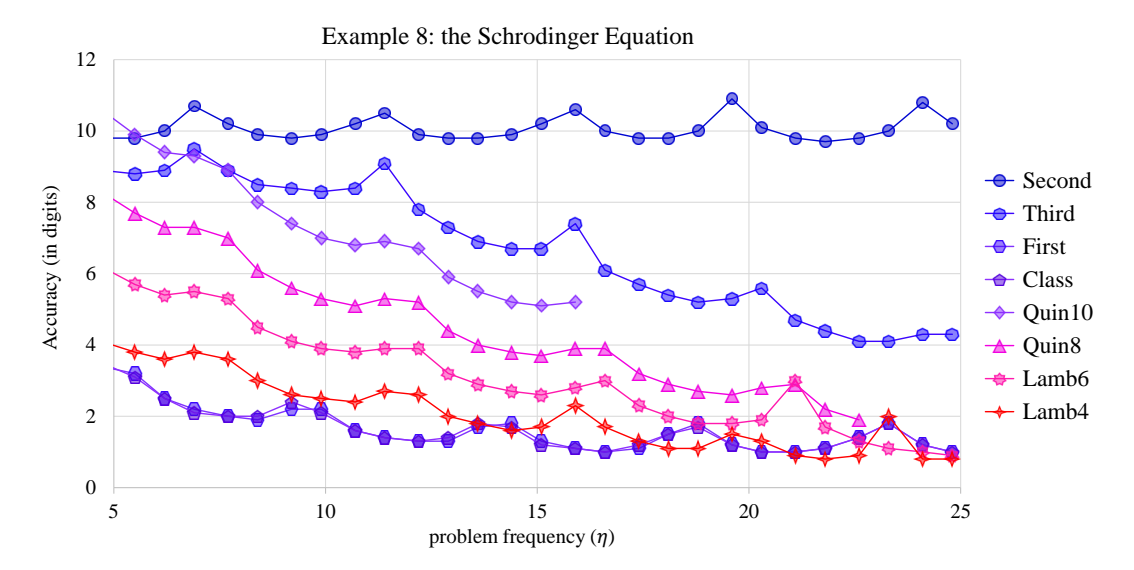


Figure 14: Curves of the accuracy of the methods versus increasing the frequency of the problem in Example 4.8.

References

- [1] A. C. Allison, The numerical solution of coupled differential equations arising from the Schrödinger equation, *J. Comput. Phys.* **6** (1970) 378–391, https://doi.org/10.1016/0021-9991(70)90037-9.
- [2] K. Mu and T. E. Simos, A Runge–Kutta type implicit high algebraic order two-step method with vanished phase-lag and its first, second, third and fourth derivatives for the numerical solution of coupled differential equations arising from the Schrödinger equation, *J. Math. Chem.* **53** (2015) 1239–1256, https://doi.org/10.1007/s10910-015-0484-8.
- [3] E. Stiefel and D. G. Bettis, Stabilization of Cowell's method, Numer. Math. 13 (1969) 154-175, https://doi.org/10.1007/BF02163234.
- [4] J. M. Franco and J. F. Palacian, High order adaptive methods of Nyström-Cowell type, J. Comput. Appl. Math. 81 (1997) 115–134, https://doi.org/10.1016/S0377-0427(97)00030-7.
- [5] J. F. Frankena, Störmer-Cowell: straight, summed and split. An overview, *J. Comput. Appl. Math.* **62** (1995) 129–154.
- [6] G. D. Quinlan and S. Tremaine, Symmetric multistep methods for the numerical integration of planetary orbits, Astron. J. 100 1694–1700.
- [7] J. D. Lambert and I. A. Watson, Symmetric multistip methods for periodic initial value problems, *J. Inst. Math. Appl.* **18** (1976) 189–202.
- [8] T. E. Simos, A new methodology for the development of efficient multistep methods for first-order IVPs with oscillating solutions, *Mathematics* **12** (2024) #504, https://doi.org/10.3390/math12040504.

- [9] J. M. Franco, I. Gómez and L. Rández, Four-stage symplectic and P-stable SDIRKN methods with dispersion of high order, Numer. Algorithms 26 (2001) 347–363, https://doi.org/10.1023/A:1016629706668.
- [10] L. Kramarz, Stability of collocation methods for the numerical solution of y'' = f(x, y), BIT **20** (1980) 215–222, https://doi.org/10.1007/BF01933194.
- [11] J. M. Franco, A 5(3) pair of explicit ARKN methods for the numerical integration of perturbed oscillators, *J. Comput. Appl. Math.* **161** (2003) 283–293, https://doi.org/10.1016/j.cam.2003.03.002.
- [12] H. Saadat, S. H. Hassan Kiyadeh, R. Goudarzi Karim and A. Safaie, Family of phase fitted 3-step second-order BDF methods for solving periodic and orbital quantum chemistry problems, J. Math. Chem. 62 (2024) 1223–1250, https://doi.org/10.1007/s10910-024-01619-3.
- [13] H. Saadat, S. H. Hassan Kiyadeh, A. Safaie, R. Goudarzi Karim and F. Khodadosti, A new amplification-fitting approach in Newton-Cotes rules to tackling the high-frequency IVPs, *Appl. Numer. Math.* 207 (2025) 86–96, https://doi.org/10.1016/j.apnum.2024.08.024.